

MODELLING OF ALUMINIUM BOX-BEAMS REINFORCED WITH UD CFRP LAMINATES

JAMES G. BROUGHTON & ALEC BEEVERS

Joining Technology Research Centre, School of Engineering - Oxford Brookes University, Gypsy Lane Campus, Headington, Oxford, UK, E-mail jgbroughton@brookes.ac.uk.

Abstract

This paper discusses recent work on the development of multimaterial structural details based on unidirectional carbon fibre-reinforced plastics (UD CFRP) adhesively bonded to thin-walled aluminium box-section extrusions. Numerical analyses have been developed to predict the performance of these structures and to identify key material properties, failure modes and structural limitations. The effects of linear-elastic and non-linear properties of the adhesive on the structural behaviour of the beams have been considered. Both experimental test and theory have demonstrated optimum performances in terms of strength, ductility and preferred failure modes by varying the thickness, stiffness or length of the CFRP reinforcing laminate and adhesive's tensile modulus.

Keywords

FE Analysis, CFRP, Adhesive bonding, Optimisation, Aluminium extrusions.

1. INTRODUCTION

Externally-bonded CFRP laminates have been used successfully for the post-strengthening of structures for over 20 years. Applications include aircraft¹, ship superstructures², bridge decks³ and blast walls⁴ in off-shore platforms. Hybrid material technology also offers unique opportunities in 'new-build' applications for the reduction of component weight. The concept of combining advanced materials with traditional materials is commonly exploited in sandwich panel technology but the technique is now being extended to other structural configurations for strengthening and reducing structural volume⁵. These may include for example side-impact bars, drive shafts and more generally for the reduction of structural volume of space frames for the transport sector.

The application considered in this study is the reinforcement of extruded aluminium beams. Two sizes of thin-walled aluminium box-section extrusions reinforced with unidirectional CFRP laminates were investigated to gain an understanding of the effectiveness of this technique in terms of enhancing flexural performance or reducing structural weight. Both experimental testing and numerical (global) modelling were used to identify key material properties, failure modes and structural limitations. Improvements in performance were investigated in terms of beam stiffness and strength. The study has also included a prediction of joint failure mechanisms for different lengths of reinforcement.

2. NUMERICAL ANALYSIS

The box-section configurations used in the study are shown in Figure 1. As each beam was symmetrical about at least two axes, the model definition was reduced to that representing just a 1/4 of the total beam section. FE analysis was initially performed to predict the load vs. mid-span deflection behaviour of the smaller (S) type extrusions followed by parametric studies to determine key material properties and geometry, and their influence on beam behaviour. Further studies were undertaken using a model of the larger beams (L) which also accommodated a prediction of joint failure, based on the attainment of peak peel stress in the adhesive. The various conditions investigated are summarised in Table 1 below.

		Parameters											
CFRP	Reinforcement								Adhesive				
Location	Thickness (mm)						Modulus (GPa)		Thickness (mm)	Modulus (GPa)	Bondline Included		
	0	0.32	0.64	1.12	1.31	4.0	148	158	0.25	2.133	Yes	No	
Asymm (S)	•	•	•		•			•				•	
Sandwich (S)		•	•		•			•				•	
Asymm (L)	•			•	•	•	•		•	•	•*		
Asymm (L)**					•		•		•	•	•		

Note: *Range of adhesive moduli from 0.001 to 10000 MPa. **All reinforcement 470mm long except for these - 3 laminate lengths of 470, 290 and 200mm were used.

Table 1 Various parameters investigated in FE modelling.

Model Verification

In order that the FE analysis could accommodate buckling and crushing of the aluminium webs and flanges a 3-D approach to the modelling was necessary. 2-D four noded shell elements were used to model the majority of the aluminium box-beam section and 3-D eight noded solid brick elements were then only required to model the transition between either one or both aluminium flanges, depending on the reinforcement configuration (see Figure 1). The solid elements extended over the whole of the flange(s) and continued 1 element thick into the web. This meant that the most critical region of stress concentrations along the adhesive bondline were located away from the transition zone, and therefore excluded the need for a more detailed model incorporating multi-point constraints (MPC). This, after verification with a fully assigned MPC model, substantially simplified the modelling.

The load was applied as a prescribed deflection to a single node 50mm in from mid-span and located on the corner of the aluminium flange and web. In the case of the sandwich reinforcement, in order to eliminate the erroneously high local stresses caused by the application of the point-load in direct contact with the CFRP, the laminate breadth fell short

of the outer edge by 1mm, allowing the load to be applied at the same location as for the asymmetric configuration. However, because of the close proximity of the CFRP to the edge of the box-section, this still resulted in localised exaggerated stresses. A solution was to restrict the two adjacent elements encompassing the point-load to that of linear-elastic behaviour.

The final mesh discretisation of a typical beam is shown in Figure 2. As the study, in some cases, involved parametric changes to the reinforcement thickness, initially the thickest laminate was modelled and subsequent models of the thinner dimensions were reproduced with the same mesh density. The various material definitions used in the FE analysis are listed in Table 2. In cases where the adhesive bondline was included the adhesive fillet was ignored and only two elements were employed to model the through-thickness of the adhesive.

Material Type	Material Definition	Material Properties
Adhesive	elasto-plastic + isotropic hardening	$E_{ADH} = 2.133$ GPa $\sigma_{YA} = 16$ MPa
Aluminium (S)	elasto-plastic + isotropic hardening	$E = 67$ GPa $\sigma_{YA} = 218$ MPa
(L)	elasto-plastic + isotropic hardening	$E = 67$ GPa $\sigma_{YA} = 185$ MPa
UD CFRP Laminate (S)	elastic orthotropic	$E_x = 158$, $E_y = 5400$, $E_z = 5400$ GPa $\nu_{xy} = 0.34$, $\nu_{xz} = 0.03$, $\nu_{yz} = 0.03$ $G_{xy} = 5000$, $G_{xz} = 5000$, $G_{yz} = 5000$ GPa
(L)	elastic orthotropic	$E_x = 148$, $E_y = 6.491$, $E_z = 6.491$ GPa $\nu_{xy} = 0.34$, $\nu_{xz} = 0.03$, $\nu_{yz} = 0.03$ $G_{xy} = 5.000$, $G_{xz} = 5.000$, $G_{yz} = 5.000$ GPa

Note: Only those figures highlighted in bold were changed in the parametric studies.

Table 2 Material properties used in the FE analysis.

3. EXPERIMENTAL

A matrix of the various beam dimensions for the two types of extrusion, used in the validation of the FE modelling, is provided in Table 3. The smaller of the two sections was selected to investigate the effect of increasing reinforcement thickness. CFRP laminates were attached either to the lower (tensile) face only, resulting in an asymmetrical cross-section, or, in a typical symmetrical sandwich configuration attached to both upper and lower flanges. All laminates were bonded to the extrusions by an ambient temperature cured epoxy adhesive.

These parametric combinations were selected to give three possible failure modes. In the mid range conditions it was expected that yield and buckling of the aluminium box-section extrusions would be the limiting factor. The thinnest reinforcements were intended to introduce tensile failure in the composite whilst the shorter reinforcement lengths were designed to induce delamination of the composite by adhesive failure.

Experimental verification of the modelling was performed with the beams tested in 4-point flexure, simply supported over a fixed span length of 500mm. The length of each beam extended over the outer rollers by 30mm, whilst the reinforcement fell short of the outer-supports in every case. Increasing mid-span deflection was applied at a rate of 2mm/min and measurements were recorded by averaging two linear-voltage displacement transducers positioned at the mid-span. A Nene Instron testing machine, fitted with a 100 kN load cell recorded the loads experienced by the test beams. Bonded strain gauges were located 5mm in from the end of the laminate on selected beams, and appropriate instrumentation was used to record strain values during incremental loading.

Reinforcement Configuration	Box-Beam Type	Box-Beam Dimensions (mm)			Beam Number	No. of Plies	Laminate Dimensions (mm)		
		height	breadth	web			Length	Breadth	Thickness
Asymmetric	Small (S)	30	20	2	01	n/a	n/a	n/a	n/a
					02	1	470	19	0.16
					03	2	470	19	0.32
					04	4	470	19	0.64
					05	8	470	19	1.31
Sandwich	Small (S)	30	20	2	06	1	470	19	0.16
					07	2	470	19	0.32
					08	4	470	19	0.64
					09	8	470	19	1.31
Asymmetric	Large (L)	50	30	3	10	n/a	n/a	n/a	n/a
					11	8	470	48	1.31
					12	8	290	48	1.31
					13	8	200	48	1.31

Table 3 Matrix of small and large test beam dimensions.

4. RESULTS

Enhancements in stiffness and strength for the smaller experimental beams, as a function of weight, are shown in Table 4. Also included are the strain measurements for the larger asymmetrical beams reinforced with the progressively shorter laminate lengths, taken 5mm in from the ends of the laminate at peak loads. The load vs. mid-span deflection characteristics of the beams are shown in Figures 3 and 4, which also include FE predictions of the flexural behaviour. Peak loads were determined by CFRP rupture, based on the attainment of maximum tensile ($X_T = 2103$ MPa) or compressive strength ($X_C = 1373$ MPa) of the laminate parallel to the fibre axis, or by buckling collapse of the box-section webs and flanges.

FE investigation into the influence of a range of adhesive moduli on beam stiffness was performed using the larger beam configuration. The resulting normalised beam stiffness (in comparison with an unreinforced control beam) is shown in Figure 5 as a function of adhesive modulus.

Reinforcement Configuration	Beam Number	Weight		Stiffness		Yield Strength (YS)		Ultimate Strength (US)		Strain at (US)
		% incr	N/mm	% incr	kN	% incr	kN	% incr	%	
Asymmetric (S)	01	0.0	550	0	2.85	0	4.37	0	n/a	
	02	1.0	610	10.9	2.92	2.5	4.73	8.2	n/a	
	03	2.0	637	15.8	3.07	7.7	5.65	29.3	n/a	
	04	3.9	691	25.6	3.20	12.3	6.43	47.1	n/a	
	05	8.0	853	55.1	3.33	15.7	6.29	43.9	n/a	
Sandwich (S)	06	2.0	631	14.7	3.28	15.1	4.74	8.5	n/a	
	07	3.9	712	29.5	3.62	27.0	5.84	33.6	n/a	
	08	8.0	830	50.1	4.37	53.3	6.54	49.7	n/a	
	09	16.0	1107	101.3	6.17	116.5	7.39	69.1	n/a	
Asymmetric (L)	10	0.0	3624	0	9.90	0	16.05	0	n/a	
	11	5.0	4651	28.3	11.86	19.8	23.08	43.8	0.051	
	12	3.1	4651	28.3	11.86	19.8	22.77	41.87	0.094	
	13	2.1	4651	28.3	11.86	19.8	16.05	0	0.094	

Table 4 Flexural performance enhancements for experimental beams.

The load vs. mid-span deflection including FE failure load predictions (based on the attainment of the peak peel stress of the adhesive) are shown in Figure 6 for the three different reinforcement lengths. Peak stress/strain values at the very end of the laminate, representative of the complete load history of the beams through ultimate conditions, are plotted in Figure 7. The resulting von Mises stress in the aluminium, along the length of the three different laminates is shown in Figure 8 and finally the longitudinal strain in the CFRP 5mm in from the laminate end is shown in Figure 9 for the test beams 11, 12 and 13.

5. DISCUSSION

Experiment

Significant improvements in performance were achieved by all the smaller reinforced beams of both asymmetric and sandwich reinforcement configuration, for increasing amounts of CFRP (see Table 4).

Comparing the two reinforcement configurations stiffness enhancement, as a function of weight, appears to be similar in both cases. The yield strength of the asymmetric beams showed the least improvements, exhibiting only 15.7% increase compared with a 53.3% increase for a sandwich beam reinforced with an equivalent amount of reinforcement. However, in both cases ultimate loads were governed by the strength of the lower laminate reinforcement, even though the sandwich beams invariably exhibited initial compressive failure of the upper laminate, beneath the point-loads. The asymmetric beams eventually reached a limit at which no further improvement was to be gained from additional CFRP reinforcement. This limit-point coincided with a change in failure mode of the beams from a

catastrophic failure, involving tensile rupture of the laminate, to that of a ductile response resulting from the collapse of the box-beam. This also corresponded with the attainment of the maximum ductility (deflection at peak load) of the beams.

Numerical

FE predictions of the flexural behaviour of the smaller beams, excluding the adhesive bondline, were found to be in excellent agreement with experiment (see Figures 4 and 5); predicted failure loads were based on the tensile or compressive strength of the laminate parallel to the fibres only.

The inclusion of the adhesive bondline into the models of the larger beams has illustrated a considerable sensitivity in the stiffness of the beams to adhesive tensile modulus. In general, increasing the adhesive modulus from 1 to 100 MPa (see Figure 6), involving either thick or thin laminate reinforcement, resulted in an increase in beam stiffness. However, an increase beyond 100 MPa provided no significant change in beam stiffness (irrespective of the CFRP laminate thickness), i.e. the reinforcement was fully effective. Whilst it is accepted that the modulus of most structural adhesives is above 100 MPa at 20°C, at temperatures above their T_g value the effects of a reduced modulus may well become important.

Despite the limitations of the global model analysis, the prediction of joint strength, based on the attainment of peak peel stress in the adhesive at the end of the laminate (see Figure 7), provided a workable estimate of joint failure loads (see Figure 8). A dramatic fall in peak peel strain is observed shortly after the peak peel stress is predicted in the shortest laminate length of 200mm (see Figures 6 and 7). This appears to signify the transfer of load in the fully plastic adhesive from the very end of the laminate which, exacerbated by the gross local yielding of the aluminium (see Figure 9), cannot sustain the load any further and initiates the delamination of the composite from the beam.

6. CONCLUSIONS

- The quasi-static flexural behaviour of aluminium box-beams can be substantially improved with UD CFRP reinforcement bonded to either one single flange or in a typical sandwich configuration.
- An optimum thickness of reinforcement has been observed and predicted using FE models. Beams reinforced with the optimum thickness provided maximum peak load and greatest ductility, whilst exhibiting the preferred (ductile) failure mode through ultimate conditions.
- Failure of the beams, involving composite rupture, has been successfully predicted using maximum longitudinal strength values of the CFRP laminate in tension and compression only.
- FE analysis indicates that reducing the tensile modulus of the adhesive below 100 MPa can significantly reduce beam stiffness. However, increasing values above 100 MPa appears to have little effect on beam stiffness.
- The stress distribution along the length of the adhesive bondline, determined by FE analysis, exhibits high stress concentrations at the end of the reinforcement, as found in lap-shear joint analysis.

- Joint failure was reasonably well determined using the attainment of peak peel stress at the end of the laminate reinforcement. The triggering of yield in the aluminium at the very end of the laminate is proposed as an indicator of imminent adhesive failure.

7. REFERENCES

1. **Baker AA**, *Repair of cracked and defective metallic aircraft components with advanced fibre composites - An overview of Australian work*, Composite Structures, Vol. 2, 1984, pp153-181.
2. **Allan RC, Bird J and Clarke JD**, *The use of adhesives in the repair of cracks in ships' superstructures*, I Mech E, Proc. - Structural Adhesives in Engineering, ISBN 0 85298 5924, 1986.
3. **Meier U and Winistorfer A**, *Retrofitting of structures through external bonding of CFRP sheets*, Non-metallic (FRP) Reinforcement of Concrete Structures, Ed. Taerwe L., Published by E and FN Spon, London No.55, 1995, pp465-472.
4. **Barnes F**, *CFRPs for strengthening and repair*, Construction and Repair, May/June, 1997, pp39-42.
5. **Broughton JG, Beevers A and Hutchinson AR**, *Carbon-fibre-reinforced plastic (CFRP) strengthening of aluminium extrusions*, Int. J. Adhesion and Adhesives, Vol.17, 1997 pp269-278.

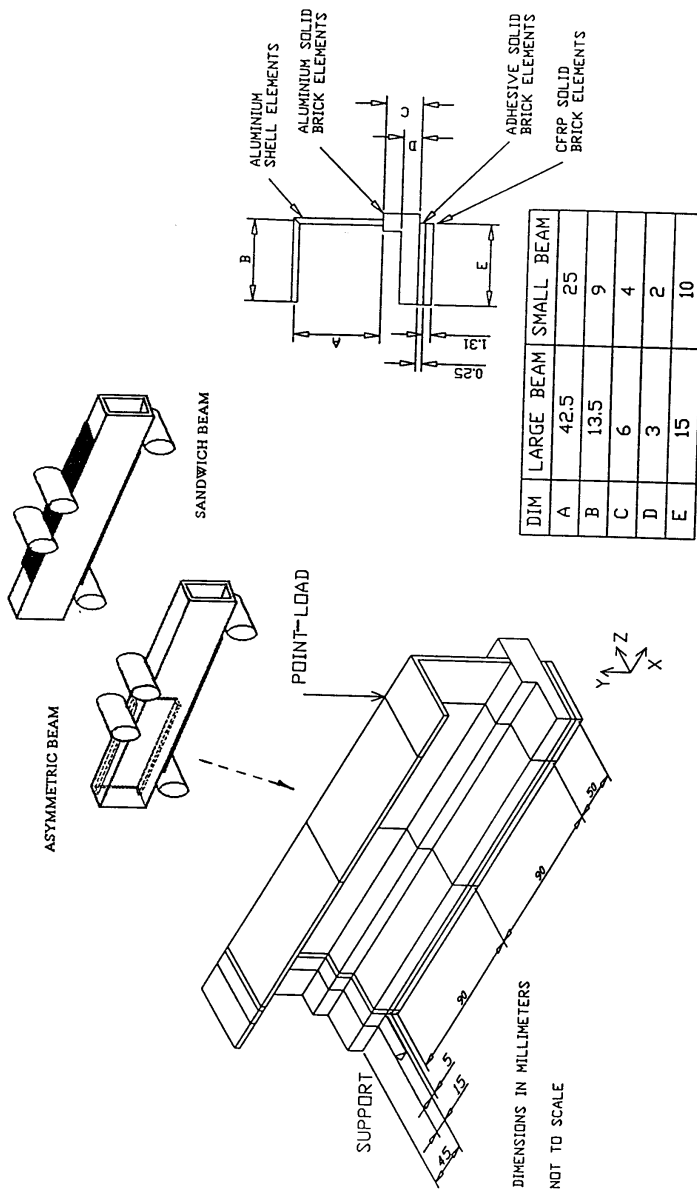


Figure 1 Beam geometry and test configuration.

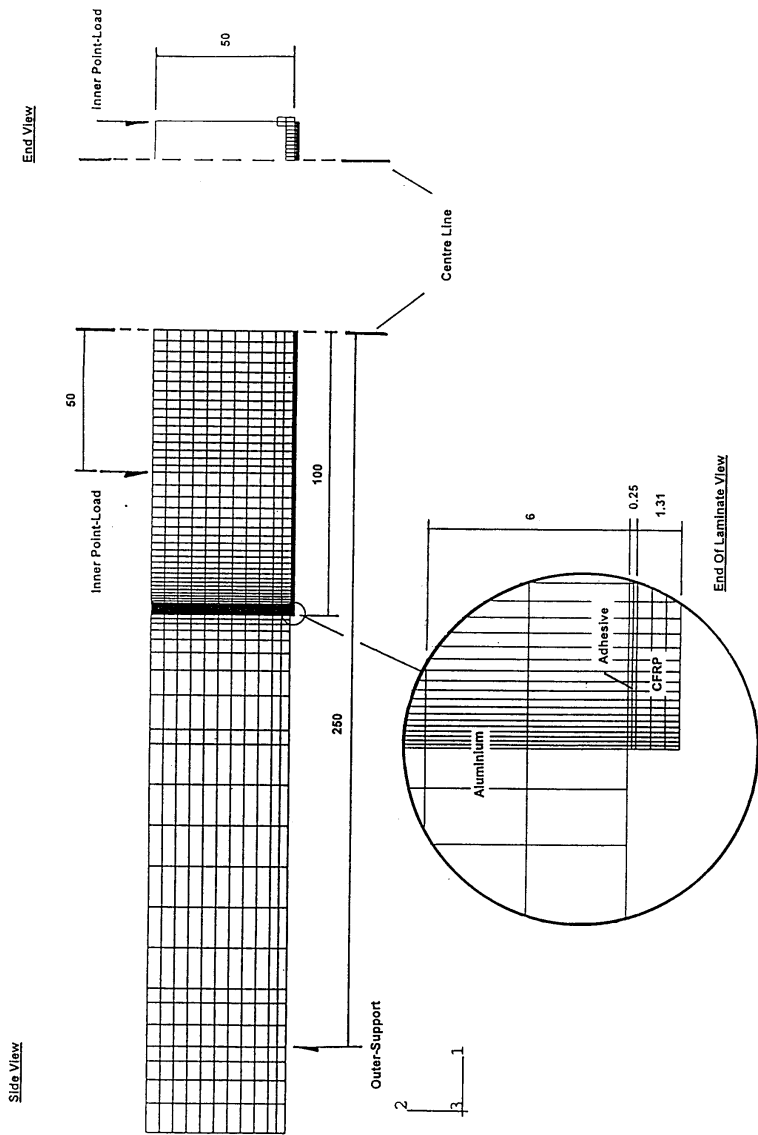


Figure 2 Mesh discretisation for beam 11.

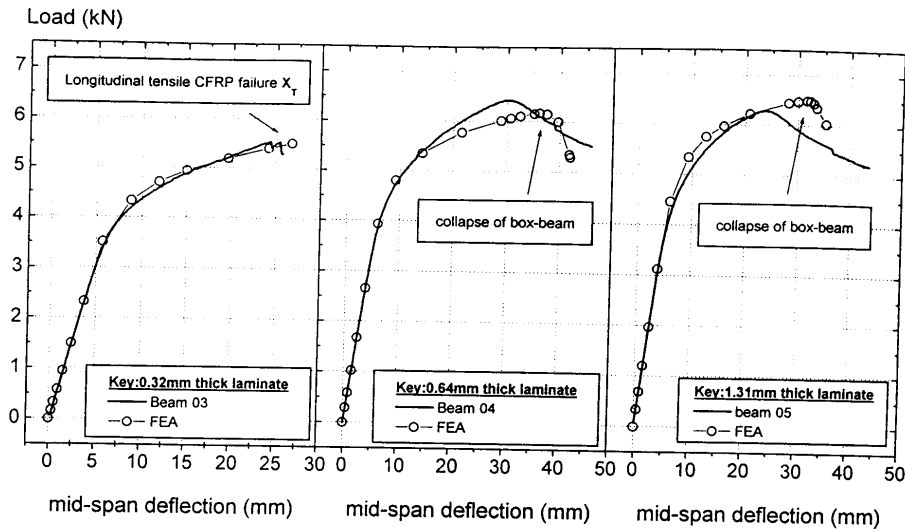


Figure 3 Load vs mid-span deflection of the smaller asymmetrically-reinforced beams

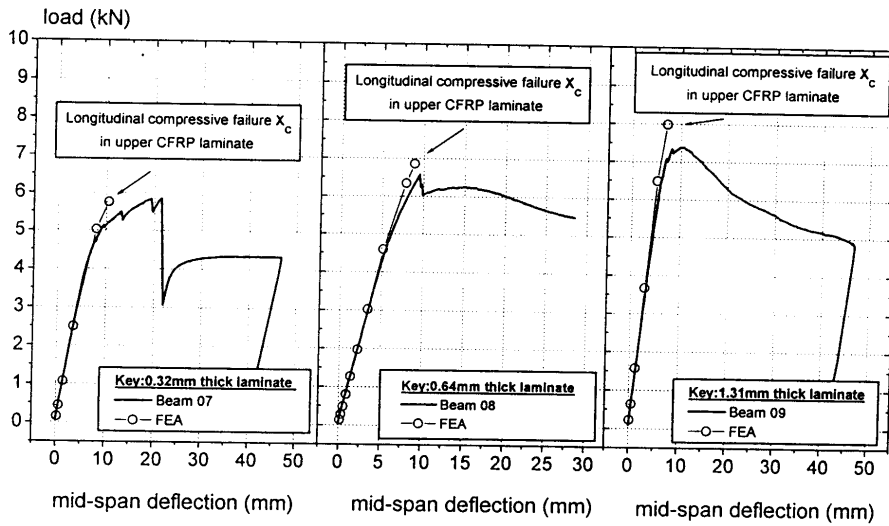


Figure 4 Load vs mid-span deflection of the smaller sandwich beams

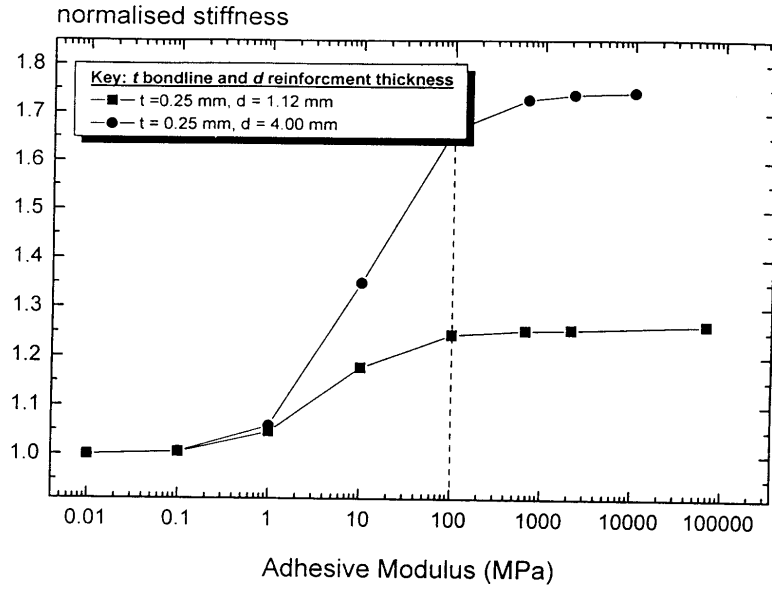


Figure 5 Predicted beam stiffness due to variations in adhesive modulus

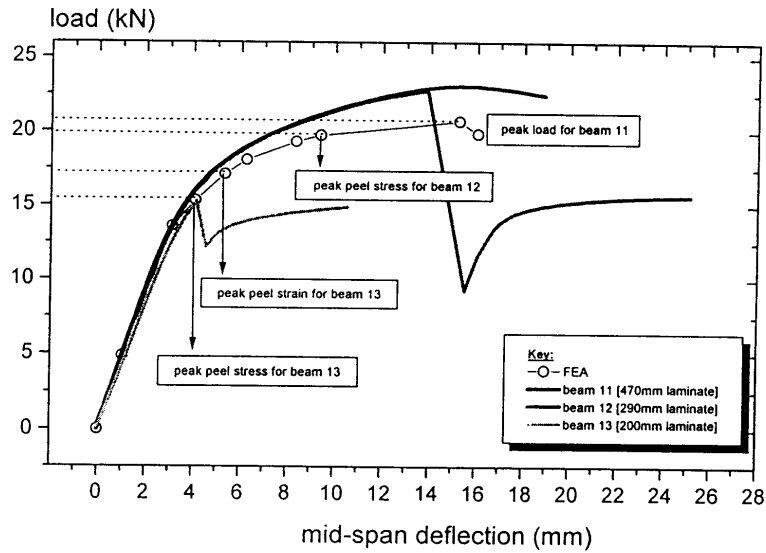


Figure 6 Load vs. mid-span deflection and predicted failure loads for the larger beams 11,12 and 13

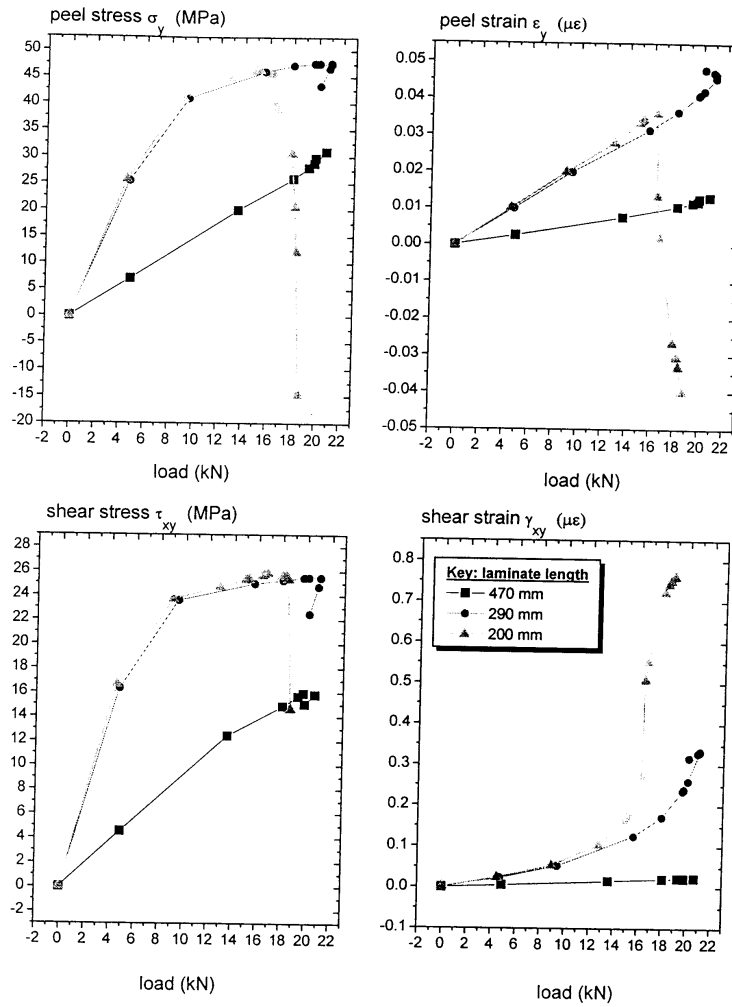


Figure 7 Predicted peak stress/strain at the end of the laminate for the different laminate lengths

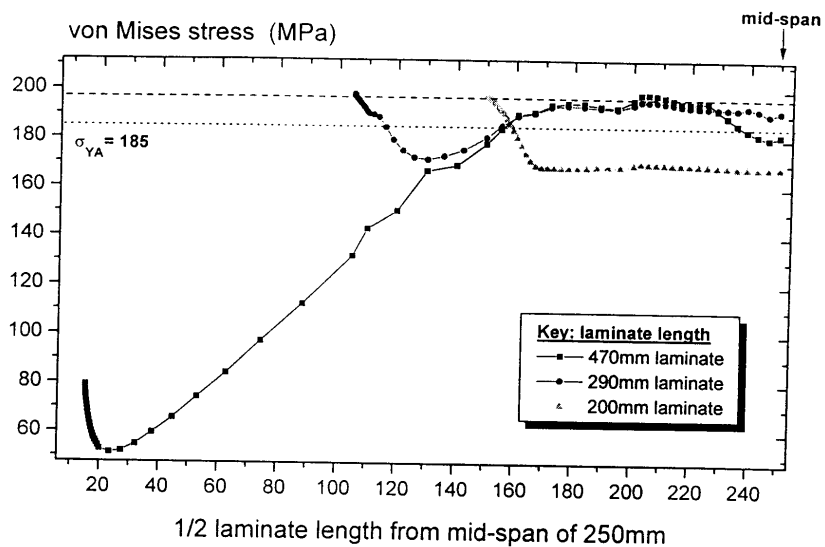


Figure 8 Von Mises stress plot in aluminium at peak loads for different laminate lengths

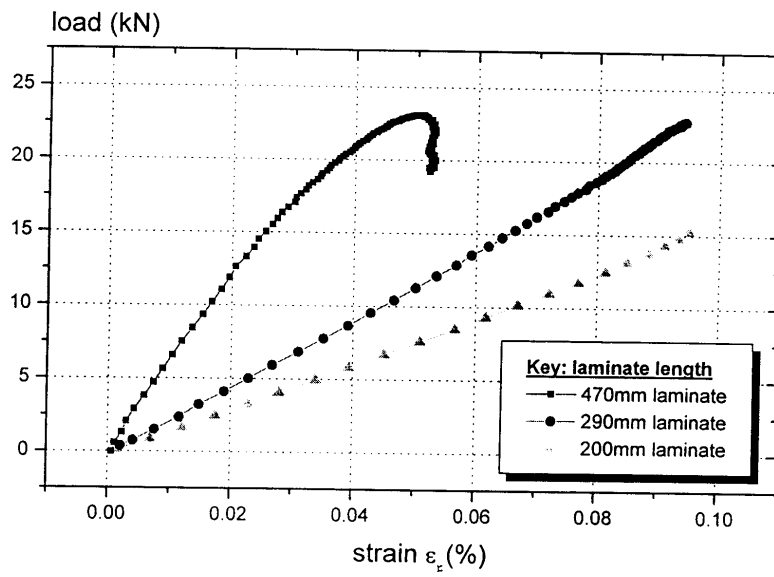


Figure 9 Strains at gauge location 5 mm from the laminate-end